catalysts

MDPI

Article

Activity of $Ag/CeZrO_2$, $Ag+K/CeZrO_2$, and $Ag-Au+K/CeZrO_2$ Systems for Lean Burn Exhaust Clean-Up

Ewa M. Iwanek (nee Wilczkowska) [1,*], Leonarda Francesca Liotta [2,*], Shazam Williams [3], Linjie Hu [3], Huitian Ju [3], Giuseppe Pantaleo [2], Alisha Thapar [1], Zbigniew Kaszkur [4], Donald W. Kirk [5] and Marek Gliński [6]

1 Faculty of Applied Science and Technology, Sheridan College, Brampton, ON L6Y 5H9, Canada; alishathapar3@gmail.com
2 Istituto per lo Studio di Materiali Nanostrutturati (ISMN)-CNR, I-90146 Palermo, Italy; giuseppe-pantaleo@cnr.it
3 DCL International Inc., Concord, ON L4K 4T5, Canada; swilliams@dcl-inc.com (S.W.); rhu@dcl-inc.com (L.H.); jju@dcl-inc.com (H.J.)
4 Institute of Physical Chemistry, Polish Academy of Sciences, 01-224 Warsaw, Poland; zkaszkur@ichf.edu.pl
5 Department of Chemical Engineering and Applied Science, University of Toronto, Toronto, ON M5S 3E5, Canada; don.kirk@utoronto.ca
6 Faculty of Chemistry, Warsaw University of Technology, 00-664 Warsaw, Poland; marek.glinski@pw.edu.pl
* Correspondence: ewa.iwanek@sheridancollege.ca (E.M.I.); leonardafrancesca.liotta@cnr.it (L.F.L.)

Abstract: Herein, the activity of Ag and bimetallic Au-Ag catalysts, supported over $Ce_{0.85}Zr_{0.15}O_2$ (CZ), was investigated in a complex stream, whose components included CO, C_3H_8, NO, O_2, and, optionally, an injection of water vapor. In such a stream, three of the possible reactions that can occur are CO oxidation, propane combustion, and NO oxidation. The aim of these studies was to explore whether silver, due to its strong affinity to oxygen, will counteract the stabilization of oxygen by potassium. The effect of the presence of potassium ions on the activity of the monometallic silver catalysts is beneficial in the complex stream without water vapor in all three studied reactions, although it is negligible in the model CO stream. It has been shown that water vapor strongly suppresses the activity of the Ag+K/CZ catalyst, much more so than that of the Ag/CZ catalyst. The second purpose of the work was to determine whether the negative effect of potassium ions on the activity of nanogold catalyst can be countered by the addition of silver. Studies in a model stream for CO oxidation have shown that, for a catalyst preloaded with gold, the effect of potassium is nulled by silver, and the activity of AuAg + 0.15 at%K/CZ and AuAg + 0.30 at%K/CZ is the same as that of the monometallic Au catalyst. Conversely, when the reaction is carried out in a complex stream, containing CO, C_3H_8, NO, O_2, and water vapor, the presence of water vapor leads to higher CO conversion as well as increased NO_2 formation and slightly suppresses the C_3H_8 combustion.

Keywords: NO oxidation; CO oxidation; propane combustion; Ag and Ag-Au bimetallic systems; potassium ion effect

Citation: Iwanek, E.M.; Liotta, L.F.; Williams, S.; Hu, L.; Ju, H.; Pantaleo, G.; Thapar, A.; Kaszkur, Z.; Kirk, D.W.; Gliński, M. Activity of $Ag/CeZrO_2$, $Ag+K/CeZrO_2$, and $Ag-Au+K/CeZrO_2$ Systems for Lean Burn Exhaust Clean-Up. *Catalysts* **2021**, *11*, 1041. https://doi.org/10.3390/catal11091041

Academic Editor: Lucie Obalová

Received: 18 July 2021
Accepted: 28 August 2021
Published: 28 August 2021

1. Introduction

Currently, gold alloyed with silver is being investigated in catalysis and electrochemistry as an interesting combination. An enhanced activity of bimetallic Au-Ag catalysts in selective alcohol oxidation [1] has been explained as the result of its impact on the dynamic restructuring of the catalyst surface which leads to an improved activity of these systems. The combination of these two metals has also shown to be beneficial in CO oxidation [2] and CO-PROX [3]. Other reactions in which Ag-Au alloys have also been applied as catalysts are glycerol oxidation [4] and aerobic oxidation of p-hydroxybenzyl alcohol [5]. In the former reaction, both gold and silver are active, but a synergistic effect of an Au-Ag alloy has been observed and attributed to an enhanced activation of oxygen. Au-Ag alloys

supported on titania [6] and Au-AgX-type systems (X = Cl, Br, I) [7] systems have been studied as photocatalysts activated by visible light. Ag-Au alloys in the form of nanoprisms have been shown to be effective catalysts in the reduction in 4-nitrophenol by $NaBH_4$ [8], which show that these systems are capable of transferring electrons, hence bringing about a reaction that does not occur at all without these particles. Another recent finding about the electron transfer by Au-Ag alloys reveals that such systems may, under appropriate synthesis conditions, exhibit superconductivity [9].

Silver is known to bind to oxygen easily, which is beneficial in CO oxidation [10]. In the case of CO oxidation or PROX, there are very few studies that employ bimetallic Au-Ag systems. The two articles mentioned above [2,3] indicate that such catalysts can be better than monometallic systems. It was found that a sequence of depositing silver before gold led to reoxidizing of the silver reduced prior to this step [2]. However, the sequential deposition of Au and Ag onto the catalyst support (alumina) has been suggested to be beneficial for hydrocarbon-SCR of NO_x [11]. Without depositing gold in one batch and adding other components later, it is difficult to completely exclude any differences between each batch, including synthesis conditions (e.g., pH), metal loading/deposition rate, etc. and compare the results of co-precipitated Au-Ag systems with monometallic Au and monometallic Ag systems. Although it is commonly known that gold catalysts need to have an average particle size of 5 nm or less to be active, Liu et al. have demonstrated that, in the case of Ag-Au alloys, particles whose size is 30 nm (much above the accepted size for monometallic gold) have been shown to be very active [12]. Therefore, one of the aims of this study was to compare the activity of two bimetallic systems with different size particles, but with the same loading of each of the metals, to determine if there is a noticeable difference in the activity of these systems.

Temperature programmed reduction is a powerful tool to gain insight of catalyst preparation and composition on its reducibility, but also to probe the mutual interaction between active metals, such as Ag and Au, and their interaction with the support. A narrow TPR signal is indicative of the reduction in species with the same chemical environment, i.e., all are similar in nature, size, strength with the support, whereas a broad signal corresponds to the reduction in different oxidized species likely differing in the oxidation state, particle size, mutual interaction, or with the support. Considering the current literature, there is a gap in the TPR studies of Au-Ag catalysts regarding a clear understanding of the impact of the presence of Ag on the interaction of Au with the support and vice versa, which this paper aims to fill. In general, monometallic silver catalysts usually have a higher T_{max} of the reduction peak and a broader signal than monometallic gold catalysts [13–15]. An increase in the silver content tends to cause the broadening of the reduction peak and its shift to lower temperatures, but not always [13,16]. In the case of results reported by Sasirekha et al., the width of the reduction peak is not a function of the silver content [13], and the narrowest peak, which has a maximum reduction rate at the lowest temperature, is that of an alloy in [7,13]. In contrast, in studies by Fiorenza et al., the reduction peak of the Au-Ag catalyst that had a lower T_{max} than the monometallic gold catalyst was broader than the peak obtained for the Au system [17]. In another study, there was no substantial effect of the composition on the width of the reduction peak, but only on the T_{max} [14]. Finally, in [16], there was no trend of either the width or T_{max} of the reduction peak on the Ag content in bimetallic catalysts. Since the activity of catalysts in CO oxidation depends on the reductivity of the system, it is paramount to limit the number of variables, which may cause differences between catalysts in a set. Starting out with one batch of support and performing one deposition of gold onto it ensures that the starting parameters are the same, and when components are added sequentially, one can hope for a meaningful interpretation of each change.

A recently published review [18] presents a thorough literature compilation about the positive influence of potassium ions on the activity of different types of catalyst in a variety of reactions, such as N_2O and NO decomposition, NH_3– and HC-SCR, NO oxidation, and soot combustion. Although the modification of gold catalysts with alkali metals has

not been widely studied, the beneficial effect of the presence of potassium ions on the activity of silver catalysts in several reactions has been shown in the presence of potassium ions [19–21]. In the gasification of coal, different metal cations exhibit different levels of mobility, and these cations are associated with a specific amount of oxygen [22,23]. However, the effect of potassium ions on the activity of a reaction does not have to be beneficial. A recent study on selective catalytic reduction in NO_x shows that the introduction of K ions reduces the number of Brönsted acid sites on the surface of the studied catalysts, which, in turn, leads to a decrease in the NO_x conversion at higher temperatures [24]. Our previously published work showed that the addition of potassium ions onto the surface of $Au/CeZrO_2$ catalysts causes a shift in the maximum temperature of the reduction peak to higher temperatures, and that this shift correlates with the loss of activity in CO oxidation [25]. Based on data thus far reported in the literature, in the present work, we have prepared Ag and bimetallic Au–Ag catalysts supported over $Ce_{0.85}Zr_{0.15}O_2$, and the second objective of this study was to investigate the effect of potassium ions on their chemical and physical properties, as well as their catalytic performance.

2. Results

In order to exclude the impact of variable support composition and properties, a large batch of a ceria-zirconia support was synthesized, dried, calcined, crushed and sieved. The support CZ has composition $Ce_{0.85}Zr_{0.15}O_2$. The same solution of silver nitrate was used to deposit silver onto the support and the support pre-loaded with gold at the same time to avoid any differences in synthesis conditions. The composition of each catalyst is presented in Table 1. Catalysts Ag/CZ and Ag+K/CZ contain only silver. The support used for making the bimetallic catalysts was pre-loaded with the gold precursor using wet impregnation, which is a commonly used technique, dried and calcined, after which it was divided into portions. Both bimetallic catalysts labelled AuAg+K/CZ contained gold (0.30 at%), silver (0.15 at%), and 0.15 at% potassium ions (Table 1), but the one with the letter (+T) had an additional thermal treatment. AuAg+2K/CZ has double content of potassium ions (0.30 at%).

Table 1. Composition and properties of the catalysts.

Symbol	Loading (at%)			S_{BET} [m^2/g]	d_p [b] [nm]	V_p [b] [cm^3/g]	d_{Au} [nm]	$a_{sup.}$ [Å]
	Au [a]	Ag	K					
Ag/CZ	N/A	0.15	N/A	75 ± 3	2.5 (2)	0.03 (1)	N/A	5.378 (1)
Ag+K/CZ	N/A	0.15	0.15	76 ± 3	2.6 (2)	0.04 (1)	N/A	5.377 (1)
AuAg+K/CZ	0.3	0.15	0.15	74 ± 3	2.6 (2)	0.03 (1)	3.5 ± 0.3	5.376 (2)
AuAg+2K/CZ	0.3	0.15	0.30	76 ± 3	2.6 (2)	0.04 (1)	3.1 ± 0.3	5.376 (2)
AuAg+K(+T)/CZ	0.3	0.15	0.15	74 ± 3	2.6 (2)	0.03 (1)	30 ± 2	5.375 (1)
Au/CZ	0.3	N/A	N/A	75 ± 3	2.5 (2)	0.03 (1)	3.6 + 0.4	5.373 (1)
Support ($Ce_{0.85}Zr_{0.15}O_2$)	N/A	N/A	N/A	75 ± 3	2.7 (2)	0.03 (1)	N/A	5.373 (1)

[a] determined using ICP; [b] pore diameter and pore volume (BJH desorption isotherm).

Figure 1 contains SEM images of the synthesized catalysts acquired at a magnification of 100,000 times. The morphology of Ag/CZ and Ag+K/CZ is the same and no particles are visible in either one (Figure 1a,b). With the average pore diameter of the support smaller than 3 nm (Table 1), it is clear that the oxide is a nanoporous material and therefore pores are not visible in the SEM images. Figure 1c–e depict the textural properties of the bimetallic samples. No visible agglomerates can be seen in these images, as in the image of the Au reference, except for the one which has been subjected to additional thermal treatment (Figure 1e), in which substantially larger Au particle sizes are detected.

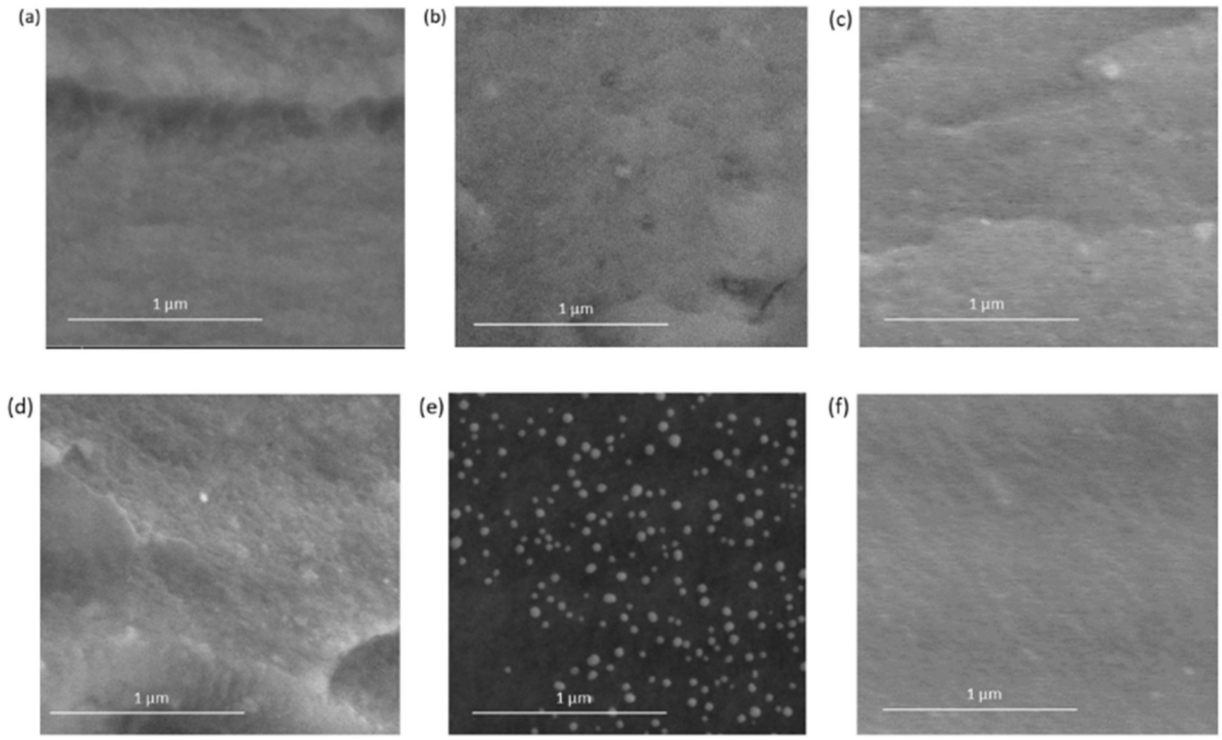

Figure 1. SEM images of silver catalysts: (**a**) Ag/CZ, (**b**) Ag+K/CZ, and the bimetallic systems: (**c**) AuAg+K/CZ, (**d**) AuAg+2K/CZ, (**e**) AuAg+K(+T)/CZ, (**f**) Au reference at the magnification of 100,000 times.

The diffraction patterns of the catalysts (Figure 2) show that the main phase present in all the systems is the same fluorite-type mixed cerium–zirconium oxide. The support lattice constant for each catalyst is given in Table 1. The values obtained for all studied systems containing Ag, especially those without gold, are slightly higher than that of the Au reference, which was prepared with the same batch of the support as the studied silver-containing catalysts, and the previously prepared series of catalysts without silver [25], for which the values fall in the range 5.3728–5.3737 (8) Å. This difference may be attributed to the interaction of silver with the oxygen from the cerium–zirconium oxide; however, it requires further investigation. In a paper recently published in *Nature* [26], it has been noted that the interaction of silver with ceria can lead to a lattice parameter of ceria higher than for bulk ceria: 5.414 Å vs. 5.411 Å.

The only other distinct signals are found in the gold-containing systems and the Au reference, which correspond to Au (111) at 38.2°, which is indicated by the arrows in Figure 2. Au (111) peak position is the same as that of the Au reference (enlargement), providing no definitive information on Ag and Au alloy formation. However, the formation of an alloy would shift this peak only by a few parts per hundredth of a degree to lower 2θ values (assuming Vegard's law) and, for small Ag concentrations, may pass unnoticed. The average particle size of the gold in samples, as determined by analysis of XRD patterns, was approximately 3 nm, except for sample AuAg+K(+T)/CZ, which, as a result of an additional thermal treatment, has a substantially larger contribution from the gold phase and an average particle size of 30 nm as per calculations performed on analysis of over 200 particles in the SEM image (Figure 1e). The Au lattice constant in all the studied catalysts when calculated based on the (111) signal gives approximately 4.08 Å, whereas the values calculated using the (200) signal give a slightly higher value, approximately 4.16 Å. This is typical for crystallites, which exhibit multiple twinning. Multiple twins are usually formed along the (111) planes and are characterized by a pronounced shift of the (200) signal towards lower scattering angles, which is associated with strong deformations in this direction. In such a case, the actual size of the crystallites is several times larger than

that resulting from the Scherrer formula (and involving the average length of the ordered rows of atoms in a given crystallographic direction). This interpretation is in line with the value obtained from the SEM image of catalyst AuAg+K(+T)/CZ. This is common for gold nanocrystals, which show high mobility and are usually not well ordered.

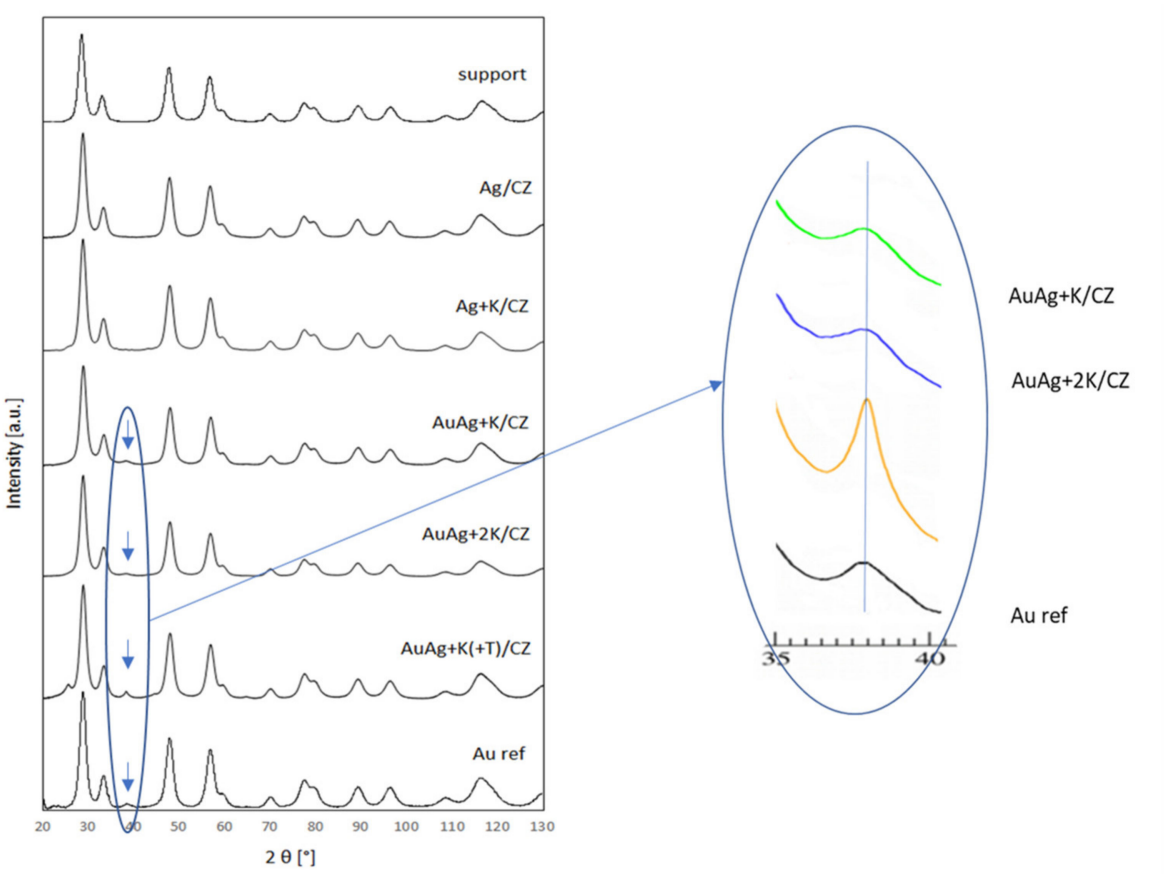

Figure 2. XRD results: diffraction patterns of the catalysts.

Figure 3 comprises the adsorption/desorption isotherms for the support loaded with potassium ions, all the studied catalysts, and the Au reference. All of them have a type 5 hysteresis loop as per IUPAC classification. It can be seen that the hysteresis loop is slightly larger for the support prior to Au and Ag deposition, but the comparison of the results obtained for the Au/Ag systems with the Au reference shows that the presence of silver does not affect the shape of the adsorption/desorption isotherms.

The survey spectra of all the catalysts indicate that the surfaces of these systems do not have any additional elements/impurities which could influence the dispersion of the deposited substances (Figure 4). Despite the fact that all catalysts were dosed with the same volume of the same solution of silver nitrate, the XPS results indicate differences in the distribution of silver on the surface. The survey spectra (Figure 4a) collected for all studied samples show that both silver catalysts have a smaller signal from silver than the bimetallic systems. Moreover, the catalyst with the largest signal from Au, namely AuAg+K(+T)/CZ, has the largest signals from Ag. This shows the impact of gold on the distribution of silver on the surface of the obtained catalysts.

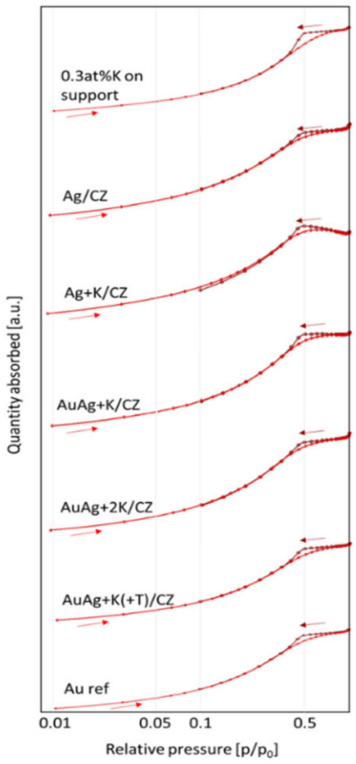

Figure 3. N_2 adsorption/desorption isotherms of the support doped with potassium ions, the studied catalysts, and Au reference sample.

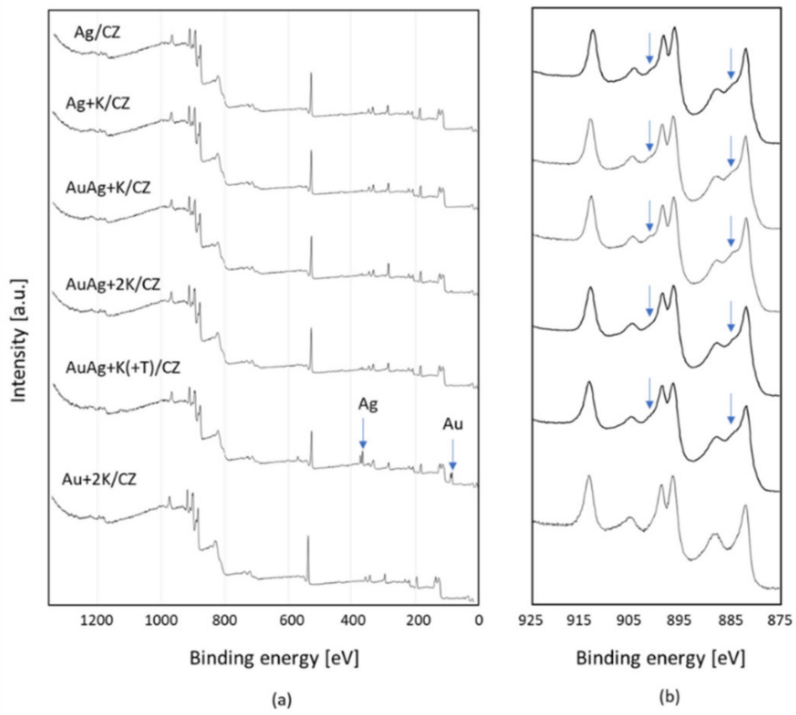

Figure 4. XPS results of all studied catalysts and Au+2K/CZ reference sample: (**a**) survey spectra and (**b**) Ce 3d detailed region.

The Ce 3d detailed region of all catalysts is shown in Figure 4b. The Ce 3d spectrum of the Au+2K/CZ catalyst shows that the cerium ions are in the 4+ oxidation state. In contrast, in the case of both monometallic silver catalysts, a contribution from the $3d^9 4f^1$(O

$2p^6)Ce^{3+}$ final state can be seen (Figure 4b arrows), which indicates that some of the surface Ce^{4+} ions are reduced to Ce^{3+}. The most pronounced effect is visible in the detailed region of AuAg+K/CZ. This component is not visible in the Au reference but can be seen in the monometallic silver and bimetallic catalysts and hence is ascribed to the presence of silver. This effect may be caused by the interaction of Ag with the oxygen of the support.

The Au 4f and Ag 3d detailed regions of the XPS spectra of the monometallic and bimetallic catalysts are compiled in Figure 5a,b, respectively. There is no substantial difference between the state of the gold in the monometallic and bimetallic catalyst. In both cases, the peaks were fitted with three components at 84.0 eV (Au^0), 85.0 eV (Au^+), and 86 eV (Au^{3+}). Table 2 contains values obtained after fitting the XPS peaks of the detailed regions of the spectra. The spin orbital splitting of the doublets were equal to: 2.8 ± 0.1 eV for K 2p, 2.35 ± 0.05 eV for Zr, 6.0 ± 0.1 eV for Ag 3d, and 3.67± 0.05 for Au 4f. From the obtained data, it can be seen that the distribution of different species of gold is similar in all systems. Therefore, it can be concluded that the sequential deposition does not allow the silver to alter the gold in a significant way.

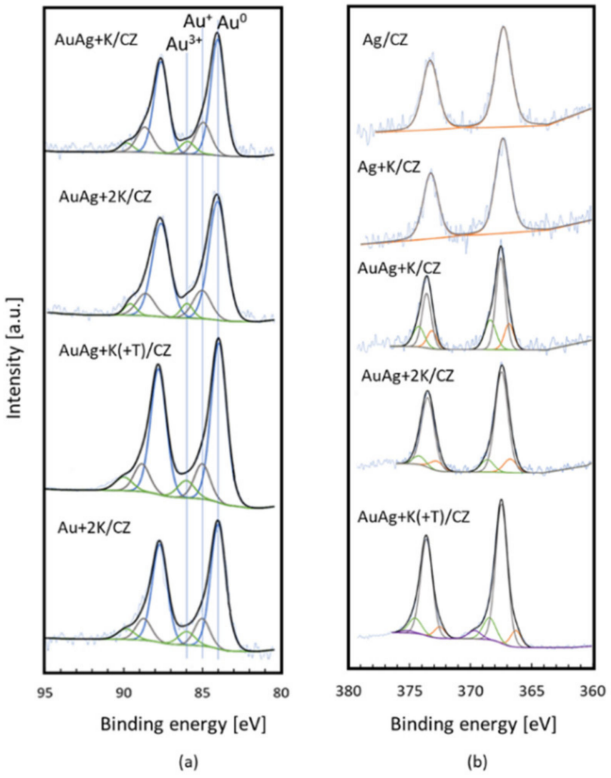

Figure 5. Detailed regions of XPS spectra: (**a**) Au 4f and (**b**) Ag3d.

For silver, the shape of the peak and the Auger parameter are said to be a better indication of the oxidation state than the binding energy of the Ag $3d_{5/2}$ peak itself [27,28]. Therefore, the Auger parameter was calculated for each catalyst and collected in Table 2. It is noticeable that there is a difference between the values obtained for the monometallic silver catalysts and those obtained for the bimetallic systems, which are accompanied by a difference in the shape. The higher Auger parameter and a symmetrical peak are typical for metallic silver [27], whereas the lower value and an asymmetric peak are associated with the presence of AgO, a salt containing both Ag^+ and Ag^{3+} ions [27,29]. The peaks were fitted accordingly. The overall amount of silver on the surface of each catalyst (Table 2) indicates that there is substantial difference in the distribution of silver, but also, to a smaller extent, of potassium ions in the case of the thermally treated sample.

The TPR curves of the studied catalysts and the Au reference, as well as that recorded for the support doped with 0.3 at% K, are presented in Figure 6. It can be seen that the curves obtained for the monometallic silver catalysts, with and without potassium, have a much broader reduction signal, which occurs at a much higher temperature (approx. 200 °C) than when gold is present. This indicates a wide range of interactions of silver with the support in the absence of gold. Moreover, both monometallic silver systems have an additional reduction peak at an intermediate temperature (at around 475 °C). It may suggest that some of the cerium–zirconium oxide is left unaffected by the presence of silver.

Table 2. XPS analysis of chemical states and atomic ratios on the surface of the studied catalysts. The numbers in brackets indicate the error of the measurement.

Symbol	Au Loading [at%]			Ag Loading [at%]	Auger Parameter [eV]	K Loading [at%]
	Au^0	Au^+	Au^{3+}			
Ag/CZ	N/A	N/A	N/A	0.42 (5)	725.9	N/A
Ag+K/CZ	N/A	N/A	N/A	0.51 (5)	726.0	0.27 (4)
AuAg+K/CZ	74.9 (9)	19.0 (9)	6.1 (9)	0.38 (5)	724.4	0.32 (4)
AuAg+2K/CZ	75.6 (9)	18.1 (9)	6.3 (9)	0.43 (5)	724.1	0.66 (4)
AuAg+K(+T)/CZ	74.8 (9)	17.4 (9)	7.8 (9)	2.74 (5)	724.3	0.82 (4)
Au+2K/CZ	74.2 (9)	17.8 (9)	8.0 (9)	N/A	N/A	0.59 (4)
support	N/A	N/A	N/A	N/A	N/A	N/A

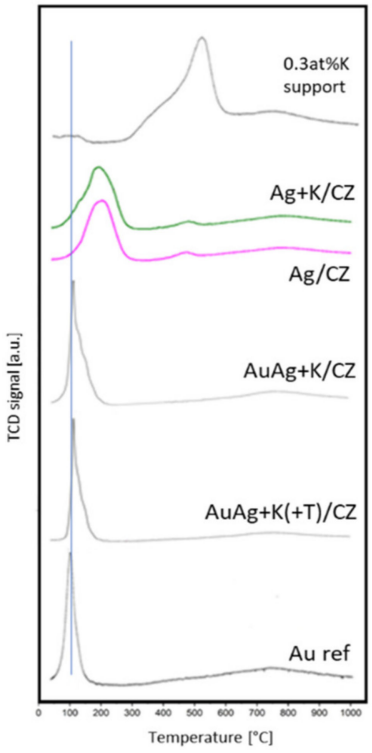

Figure 6. TPR profiles of the support doped with 0.3 at% K, the studied catalysts and the Au reference.

A similar curve, though with a slightly less symmetrical first reduction peak, but also containing a mid-temperature peak, is obtained when potassium ions are deposited onto the silver catalyst. The signals for the bimetallic systems are narrower, but the presence of Ag affected the shape of the high temperature shoulder of the reduction peak. The maximum of the reduction peak of the TPR curves of bimetallic catalysts is lower than that

of the silver catalyst, but slightly higher than that of the Au reference. It is also noteworthy that there is no mid-temperature reduction signal for the gold-containing systems. Despite the different shapes of TPR curves, the overall hydrogen consumption values measured for the investigated catalysts were comparable (1.5 mmol H_2/g). This finding suggests that the overall extent of Ce^{4+} reduction is around 60% for all studied catalysts, and that the hydrogen consumption ascribable to the reduction in any gold or silver species is negligible, due to low metal loadings.

A compilation of the activity of the studied systems in CO oxidation in both types of tests is presented in Figure 7. Figure 7a contains CO conversion values in a model oxidation stream. Au is known to be active at low temperatures in CO oxidation. It can be seen that the lowest activity is noted on the monometallic silver catalyst. The presence of potassium does not influence the activity of silver under such conditions. The activity of AuAg+K/CZ and AuAg+2K/CZ is very similar to that of the Au reference despite the fact that they contain 0.15 at% and 0.30 at% potassium ions, respectively. In short, the presence of potassium ions does not substantially impact the activity of the bimetallic catalysts. This is different than for the monometallic gold catalyst reported in [25]. This study shows that the beneficial effect of silver on the availability of oxygen counters the negative effect that is exhibited by potassium alone. The bimetallic system with large gold particles shows a substantially lower activity at higher temperatures than the other ones (Figure 7a). In studies carried out by Liu et al. [12], the activity of the monometallic silver and gold catalysts were comparable at temperatures higher than 400 °C in a model stream with 1% CO in air, whereas, at lower temperatures, the alloys were much more active than both monometallic systems, and all showed the same conversion at 475 °C. This is interesting in light of the results presented in this paper, in which the silver catalysts are substantially less active than the other systems, whereas the monometallic gold catalyst is very active. For the systems reported in the literature, the TPR curves of the bimetallic systems that exhibit superior activity to the monometallic gold catalyst usually show a better reducibility of the bimetallic system [7,13,25]. There is, however, no consensus as to how silver impacts the reducibility of Ag-Au catalysts. Some studies show a trend of shifting to lower T_{max} values with the increase in the Au content for some supports, such as ZnO [22], whereas those in which TiO_2 [10] and CeO_2 [13] were used as the supports do not.

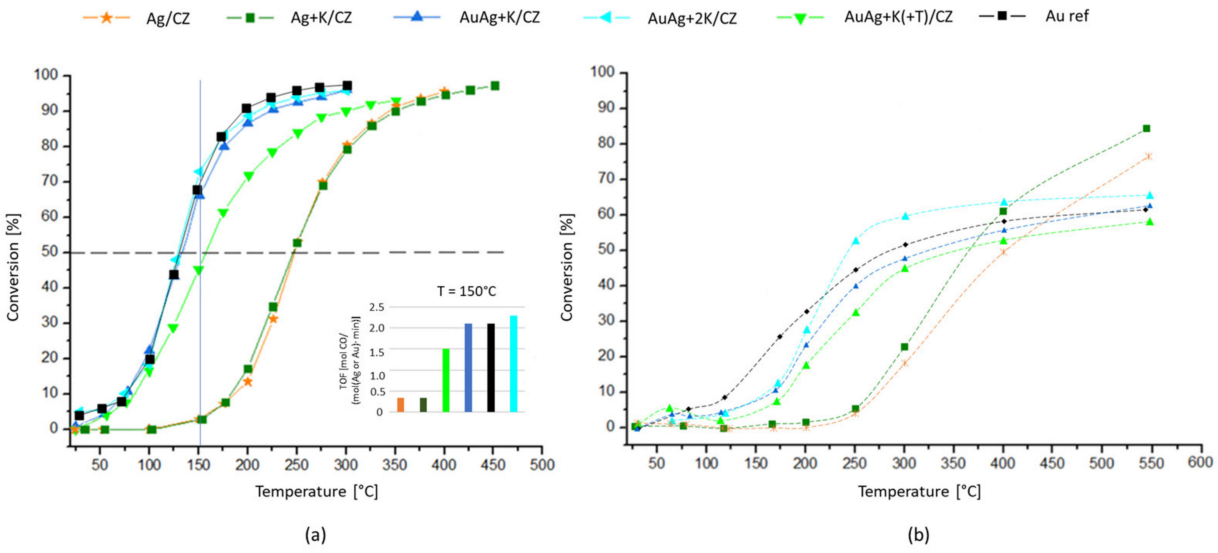

Figure 7. Activity results: CO conversion on catalysts in (**a**) a model stream, and (**b**) in a complex reagent stream without water; inset: TOF value calculated for 150 °C for the model stream using either Ag for monometallic silver system or Au for bimetallic systems.

With only 7% conversion of CO for both the monometallic silver catalysts noted at 150 °C, compared to values of approximately 70% for all the gold-containing systems, it was concluded that, at this temperature, the effect of silver in the bimetallic systems is not in substantial conversion of CO, but in assisting Au in CO conversion, as the literature suggests. This is further evidenced by the fact that the conversion on both the monometallic Au catalyst and AuAg+K/CZ is the same, which means that calculation of TOF using both available Au and Ag sites gives an artificially created difference, lowering the TOF value of the bimetallic system. This is the reason why the TOF values for monometallic silver catalysts were calculated based on the available Ag sites and those for the gold-containing systems were obtained using only the available Au sites. The value calculated for AuAg+K(+T)/CZ is smaller than those of the other gold-containing systems, which is understandable considering the lower activity of larger gold clusters.

The conversion of CO obtained for the catalysts tested in the complex stream is shown in Figure 7b. The stream also contained CO_2, hydrocarbons and NO. In such a system, there are numerous reactions, such as CO+NO, which can occur on Au [30], and processes such as NO adsorption on Ag or the support, or both, which can take place [31]. The outcome is that the monometallic Au catalyst is superior at lower temperatures, but at temperatures above 250 °C, the bimetallic system with 0.30 at% potassium exhibits higher activity (Figure 7b), though the bimetallic system with 0.15 at% potassium ions exhibits similar activity to the monometallic gold catalyst. The activity of the catalysts that contain gold and are more active at lower temperatures levels off, and at the highest studied temperature, 550 °C, the conversion of CO is practically the same as that noted at 400 °C. If the effect is due to deposition of carbon on the surface of the catalyst, then the fact that the catalyst with 0.30 at% potassium ions is better than AuAg+K/CZ and the Au reference can be explained since K^+ is a known catalyst of soot combustion. It is noteworthy that, in our previously performed studies, in a complex stream that contained water vapor, there was no levelling off of the conversion curves, but a steady, substantial increase in activity with temperature [25]. In contrast to the catalysts that contain gold, the monometallic silver catalysts are not active at low temperatures, but the increase in activity with the increase in temperature is steep. Nevertheless, in a stream without water vapor, the catalyst with potassium ions exhibited a higher activity than Ag/CZ (Figure 7b).

Figure 8 contains the activity of the catalysts in three reactions that occur in the complex stream, namely: propane combustion, CO oxidation, and NO_2 formation, for three selected systems: Ag/CZ, Ag+K/CZ, and AuAg+K/CZ. The results of tests carried out without water vapor in the stream are shown on the left panel and those of tests with water vapor are shown on the right-hand side. In the case of propane combustion (Figure 8a) in a steam without water vapor, all three systems have a similar activity at 200, 300, and 400 °C. At 550 °C, there is a clear difference between the activity of the two monometallic silver catalysts and that of the bimetallic system. In propane combustion, Ag/CZ is much more active than Ag+K/CZ in a stream without water. In short, the presence of potassium ions leads to lower propane conversion when there is no injection of water to the inlet stream. It is noteworthy that, when the inlet stream contains water vapor, the loss of activity is much smaller in the case of the silver catalyst with potassium ions than for the undoped silver catalyst. In contrast, the bimetallic systems in propane combustion in the complex stream exhibit practically the same activity with and without the addition of water vapor in the stream.

The CO oxidation studies indicate that also in this reaction the activity of the monometallic silver catalyst without potassium ions is strongly suppressed in the presence of water vapor (Figure 8b). In contrast, the activity of the monometallic silver catalyst with potassium ions is unaffected by water vapor. Its activity in both streams is the same at all studied temperatures. It is noteworthy that, in the case of the bimetallic system, the activity improves upon the addition of water vapor to the inlet stream.

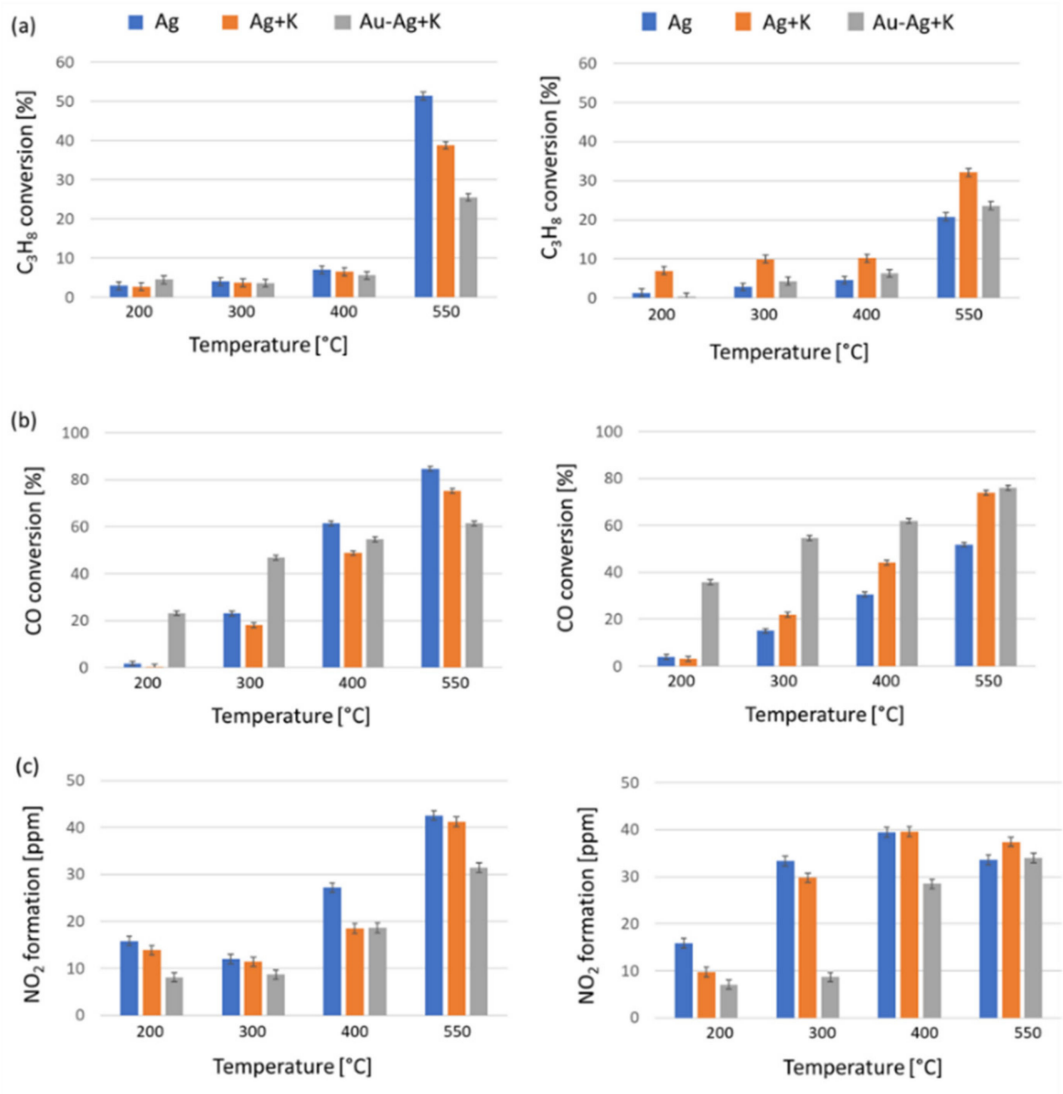

Figure 8. Activity results for Ag/CZ, Ag+K/CZ, and AuAg+K/CZ in complex stream: (**a**) C_3H_8 combustion, (**b**) CO oxidation, and (**c**) NO_2 formation without (left) and with water vapor (right) in the inlet stream.

In a complex stream that contains NO, the formation of NO_2 is possible. Figure 8c compiles the values (in ppm) of NO_2 that formed at 200, 300, 400, and 550 °C. In this reaction, the undoped monometallic silver catalyst has a higher activity in the presence of water vapor than in a stream without it at the three lower temperatures. The silver catalyst doped with potassium also exhibits a pronounced increase in activity at the three lower temperatures upon the addition of water vapor to the stream. The results indicate that there is less NO_2 formed in the presence of the bimetallic system than on Ag/CZ and Ag+K/CZ, except for one temperature, in the stream without water vapor. It should be emphasized that the formation of NO_2 occurs to a smaller extent on the bimetallic system than on the monometallic silver catalyst under all studied conditions except in the presence of water vapor at 550 °C, at which the activity of these two systems is the same.

3. Materials and Methods

3.1. Support and Catalyst Synthesis

The cerium–zirconium mixed oxide with composition $Ce_{0.85}Zr_{0.15}O_2$ was prepared as described previously [25]. In brief, the two precursors, namely ammonium ceric nitrate (analytical grade, BDH, Randor, PA, USA) and zirconyl nitrate (analytical grade, Fisher, Ottawa, ON, Canada) were dissolved in water in a 1:7 (by weight) ratio. The sup-

port precursor was precipitated using ammonium hydroxide (analytical grade, Caledon, Georgetown, ON, Canada). After the support was filtered, dried, and calcined (550 °C, 4 h), the pellets were crushed and sieved to obtain the 100–200 μm fraction. Next, gold and silver were deposited in sequence using the following precursors $HAuCl_4 \cdot H_2O$ (analytical grade, Sigma-Aldrich, Oakville, ON, Canada) and $AgNO_3$ (analytical grade, Sigma-Aldrich, Oakville, ON, Canada). After impregnation (wet impregnation) with the gold precursor (0.3 at%), the precipitate was washed to remove chloride ions, dried, and calcined at 550 °C for 3 h, and its composition was confirmed using ICP; the procedure is given in [25]. A part of the obtained batch was put aside and used as the Au reference sample, as well as for the preparation of the reference Au+2K sample (potassium ions deposited as described below). Next, 1 mL of 0.1 M solution of $AgNO_3$ was used for 4 g of the catalyst to obtain a loading of 0.15 at% (dry impregnation). Finally, the catalysts were dosed with 0.5 mL of potassium carbonate solution obtained using 0.7 g of K_2CO_3 (analytical grade, Fisher, Ottawa, ON, Canada) dissolved in 50.00 mL deionized water to obtain 0.15 at% loading with potassium ions or twice that volume in the case of AuAg+2K/CZ to obtain a loading of 0.30 at%. All three catalysts were then calcined at 550 °C for 4 h. The deposition of Au, Ag and K did not alter the grain size. The catalyst AuAg+K(+T)/CZ was prepared in the same way, but with the calcination following the Au deposition extended to 6h in order to obtain larger gold particles.

3.2. Support and Catalyst Characterization

The supports and catalysts were imaged with a Quanta FEG 250 Secondary Emission Microscope (Field Electron and Ion Company, FEI, Hillsboro, OR, USA). They were acquired at a working distance of 11 mm, spot size 2, and beam energy 10 kV. For each sample, images were collected at magnifications of 5000, 10,000, and 20,000 times.

The nitrogen physisorption analyses were performed with a Micromeritics ASAP 2020 instrument (Micromeritics Instrument Corp., Norcross, GA, USA) after outgassing of samples (0.5–1 g of sample) for 30 min at 150 °C under vacuum. The measurements were carried out at the temperature of liquid nitrogen (77 K) with a p to p_0 ratio from 0.01 to 1.0. The specific surface area and the mean pore diameter were determined based on the Brunauer–Emmett–Teller equation and the desorption curve using the BJH model, respectively.

The elemental analysis of the surface of the samples was performed using X-ray photoelectron spectroscopy (XPS). The spectra were collected using K-Alpha from Thermo Scientific (Waltham, MA, USA). Al Kα was used as the radiation source. The pass energy of the survey spectra and detailed spectra was 200 (1 eV step) and 50 eV (0.1 eV step), respectively. In the case of the supports, only the C 1s (extended to 305 eV to include the K 2p doublet), O 1s, Ce 3d, and Zr 3d, in case of the ceria–zirconia, were acquired. For the catalysts, additionally, the Au 4f and Ag 3d detailed regions were scanned (15 scans each). The peaks were fitted with components once the background had been subtracted and after calibration to C 1s (285.0 eV).

Temperature programmed reduction (TPR) measurements were performed for all supports and catalysts on Autochem 2910 (Micromeritics Instrument Corp., Norcross, GA, USA) equipped with a thermal conductivity detector (TCD). The pretreatment consisted of heating the sample (0.1g) to 150 °C (10 °C min^{-1}) in a flow of 5% vol O_2 in He gas mixture (30 mL min^{-1}), maintaining the temperature for 10 min and cooling down the sample in helium (30 mL·min^{-1}). Next, TPR analyses were carried out by flowing a stream with composition 5 vol% H_2 in Ar (30 mL·min^{-1}) from rt to 1050 °C (10 °C min^{-1}). The hydrogen consumption values, calculated by applying proper calibration curves to the reduction peaks generated by the TCD signal, were used to estimate the reduction percent of Ce during the measurements.

The diffraction patterns of the supports and catalysts were acquired with a D5000 horizontal goniometer (Bruker AXS GmbH, Karlsruhe, Germany). The following parameters were used—anode sealed tube: Cu (Kα radiation, 1.5418 Å, 40 kV, 40 mA), beam optics:

divergent Bragg–Brentano, detector: LynxEye. Each XRD measurement encompassed the range of scattering angle from 20 to 130°. The data were analyzed as in [25].

3.3. Activity Measurements

Activity measurements in a model stream (1 vol% CO + 1 vol% O_2 in He) were conducted in a tubular quartz glass reactor with a flow of 100 mL·min^{-1} in the temperature range 25–600 °C, using 100 mg of the catalyst (Weight Hourly Space Velocity (WHSV) = 60,000 mL·g^{-1}·h^{-1}). The CO conversion was determined based on the concentration of CO and CO_2 gases monitored via an IR analyzer (ABB Uras 14, Zurich, Switzerland).

Catalytic tests in the complex stream (1.5 L/min) containing 1000 ppm CH_4, 150 ppm C_2H_6, and 50 ppm C_3H_8, 200 ppm NO, 1000 ppm CO, 5% CO_2, 10% O_2, and balanced with N_2 were carried out using 0.5 g catalyst (Weight Hourly Space Velocity (WHSV) = 180,000 mL·g^{-1}·h^{-1}). The concentration of these compounds, as well as that of NO_2, in the post-reaction mixture was determined based on the readings of a continuous gas analyzer (MultiGas 2030 FTIR, MKS Instruments Inc., Rochester, NY, USA).

All the activity tests were performed in a vertical, commercially available tubular quartz-glass reactor fitted inside a stainless steel tube equipped with a heating jacket used for small scale testing. The catalyst was placed in the middle of the reactor on glass wool and covered with glass wool. This ensured uniform distribution of the reactants across the catalyst bed. The conversion values were registered in the range of temperature, 25–600 °C, under steady-state conditions. The absence of any mass or heat transfer effect was checked by repeating tests at constant WHSV, by halving the flow rate and the mass of catalyst. The reproducibility of data confirmed the chemical regime.

4. Conclusions

A novel approach of loading pre-loaded gold ceria–zirconia catalysts with both silver, which is known to provide oxygen to gold, and potassium ions, which stabilize oxygen, revealed that the positive effect of silver successfully counteracts that of potassium, leading to the same CO conversion for both the Au-Ag+K/CeZr and Au-Ag+2K/CeZr catalysts in the model stream. However, their activity was slightly lower than that of undoped Au/CeZr, which had a lower T_{max} of the low temperature reduction peak. The results of the characterization studies have shown that the deposition of silver and potassium ions onto a catalyst pre-loaded with gold does not influence the chemical state of gold. However, there is a strong dependence of the distribution and chemical form of silver on the support depending on whether gold is present and on the gold particle size. Moreover, it has been demonstrated that the silver interacts with the oxygen from the support, leading to the reduction in Ce^{4+} to Ce^{3+} on the surface of the catalyst, and the presence of gold enhances this interaction. The activity studies in a mixed stream have shown that the presence of potassium ions in a monometallic silver system leads to lower conversion of CO and propane in a stream without water, but the Ag+K/CeZr system shows superior resistance to suppression of activity by water than the Ag/CeZr system. In contrast, no detrimental effect of water was observed on the activity of Au-Ag+K/CeZr, and a clearly positive effect on CO oxidation, especially at low temperatures, as well as in NO formation above 400 °C, occurs.

Author Contributions: Conceptualization, E.M.I., L.F.L., M.G., S.W. and L.H.; formal analysis, Z.K., L.F.L., G.P. and E.M.I.; investigation, A.T., L.F.L., G.P., E.M.I., L.H. and H.J.; resources, D.W.K. and E.M.I.; data curation, E.M.I., Z.K., L.F.L. and G.P.; writing—original draft preparation, E.M.I.; writing—review and editing, L.F.L., G.P., D.W.K., M.G., L.H. and H.J.; visualization, E.M.I. and Z.K.; project administration, E.M.I. and L.F.L.; funding acquisition, E.M.I., S.W. and D.W.K. All authors have read and agreed to the published version of the manuscript.

Funding: This research was funded by the Natural Sciences and Engineering Research Council of Canada, grant number 523834-18.

Acknowledgments: We would also like to thank Ilya Gourvich from the Centre for Nanostructure Imaging (CNI) at the University of Toronto for performing the SEM-EDX measurements, as well as Peter Brodersen from the Ontario Centre for the Characterization of Advanced Materials (OCCAM) for the X-Ray Photoelectron Spectroscopy measurements and Nunzio Gallì (ISMN-CNR, Palermo, Italy) for performing nitrogen physisorption analyses.

Conflicts of Interest: The authors declare no conflict of interest.

References

1. Zugic, B.; Wang, L.; Heine, C.; Zakharov, D.N.; Lechner, B.A.J.; Stach, E.A.; Biener, J.; Salmeron, M.; Madix, R.J.; Friend, C.M. Dynamic restructuring drives catalytic activity on nanoporous gold–silver alloy catalysts. *Nat. Mater.* **2017**, *16*, 558–564. [CrossRef] [PubMed]
2. Sandoval, A.; Delannoy, L.; Méthivier, C.; Louis, C.; Zanella, R. Synergetic effect in bimetallic Au–Ag/TiO_2 catalysts for CO oxidation: New insights from in situ characterization. *Appl. Catal. A Gen.* **2015**, *504*, 287–294. [CrossRef]
3. Fiorenza, R.; Spitaleri, L.; Gulino, A.; Sciré, S. High-Performing Au-Ag Bimetallic Catalysts Supported on Macro- Mesoporous CeO_2 for Preferential Oxidation of CO in H_2-Rich Gases. *Catalysts* **2020**, *10*, 49. [CrossRef]
4. Jouve, A.; Nagy, G.; Somodi, F.; Tiozzo, C.; Villa, A.; Balerna, A.; Beck, A.; Evangelisti, C.; Prati, L. Gold-silver catalysts: Effect of catalyst structure on the selectivity of glycerol oxidation. *J. Catal.* **2018**, *368*, 324–335. [CrossRef]
5. Chaki, N.K.; Tsunoyama, H.; Negishi, Y.; Sakurai, H.; Tsukuda, T. Effect of Ag-Doping on the Catalytic Activity of Polymer-Stabilized Au Clusters in Aerobic Oxidation of Alcohol. *J. Phys. Chem. C* **2007**, *111*, 4885–4888. [CrossRef]
6. Zielinska-Jurek, A.; Kowalska, E.; Sobczak, J.W.; Lisowski, W.; Ohtani, B.; Zaleska, A. Preparation and characterization of monometallic (Au) and bimetallic (Ag/Au) modified-titania photocatalysts activated by visible light. *Appl. Catal. B Environ.* **2011**, *101*, 504–514. [CrossRef]
7. Naya, S.; Fujishima, M.; Tada, H. Synthesis of Au–Ag Alloy Nanoparticle-Incorporated AgBr Crystals. *Catalysts* **2019**, *9*, 745. [CrossRef]
8. Kim, M.; Lee, K.Y.; Jeong, G.H.; Jang, J.; Han, S.W. Fabrication of Au–Ag Alloy Nanoprisms with Enhanced Catalytic Activity. *Chem. Lett.* **2007**, *36*, 1350–1351. [CrossRef]
9. Dalai, M.K.; Singh, B.B.; Sethy, S.K.; Sahoo, S.; Bedanta, S. Superconductivity in Ag implanted Au thin film. *Phys. Rev. B Condens. Matter* **2021**, *601*, 412607. [CrossRef]
10. Grabchenko, M.V.; Mamontov, G.V.; Zaikovskii, V.I.; La Parolad, V.; Liotta, L.F.; Vodyankina, O.V. The role of metal–support interaction in Ag/CeO_2 catalysts for CO and soot oxidation. *Appl. Catal. B Environ.* **2020**, *260*, 118–148. [CrossRef]
11. More, P.M.; Nguyen, D.L.; Dongare, M.K.; Umbarkar, S.B.; Nuns, N.; Girardon, J.-S.; Dujardin, C.; Lancelot, C.; Mamede, A.-S.; Granger, P. Rational preparation of Ag and Au bimetallic catalysts for the hydrocarbon-SCR of NO_x: Sequential deposition vs. coprecipitation method. *Appl. Catal. B Environ.* **2015**, *162*, 11–20. [CrossRef]
12. Liu, J.-H.; Wang, A.-Q.; Chi, Y.-S.; Lin, H.-P.; Mou, C.-Y. Synergistic Effect in an Au-Ag Alloy Nanocatalyst: CO Oxidation. *J. Phys. Chem B* **2005**, *109*, 40–43. [CrossRef]
13. Sasirekha, N.; Sangeetha, P.; Chen, Y.-W. Bimetallic Au−Ag/CeO_2 Catalysts for Preferential Oxidation of CO in Hydrogen-Rich Stream: Effect of Calcination Temperature. *J. Phys. Chem. C* **2014**, *118*, 15226–15233. [CrossRef]
14. AbdelDayem, H.M. Interplay between Silver and Gold Nanoparticles in Production of Hydrogen from Methanol. *Johnson Matthey Technol. Rev.* **2015**, *59*, 303–312. [CrossRef]
15. Masoud, N.; Delannoy, L.; Calers, C.; Gallet, J.-J.; Bournel, F.; de Jong, K.P.; Louis, C.; de Jongh, P.E. Silica-Supported Au–Ag Catalysts for the Selective Hydrogenation of Butadiene. *ChemCatChem* **2017**, *9*, 2418–2425. [CrossRef] [PubMed]
16. Sandoval, A.; Aguilar, A.; Louis, C.; Traverse, A.; Zanella, R. Bimetallic Au–Ag/TiO_2 catalyst prepared by deposition–precipitation: High activity and stability in CO oxidation. *J. Catal.* **2011**, *281*, 40–49. [CrossRef]
17. Fiorenza, R.; Crisafulli, C.; Condorelli, G.G.; Lupo, F.; Scire, S. Au–Ag/CeO_2 and Au–Cu/CeO_2 Catalysts for Volatile Organic Compounds Oxidation and CO Preferential Oxidation. *Catal. Lett.* **2015**, *145*, 1691–1702. [CrossRef]
18. Xu, Z.; Li, Y.; Shi, H.; Lin, Y.; Wang, Y.; Wang, Q.; Zhu, T. Application Prospect of K Used for Catalytic Removal of NO_x, CO_x, and VOCs from Industrial Flue Gas: A Review. *Catalysts* **2021**, *11*, 419. [CrossRef]
19. Chen, X.; Chen, M.; He, G.; Wang, F.; Xu, G.; Li, Y.; Zhang, C.; He, H. Specific Role of Potassium in Promoting Ag/Al_2O_3 for Catalytic Oxidation of Formaldehyde at Low Temperature. *J. Phys. Chem. C* **2018**, *122*, 27331–27339. [CrossRef]
20. Bai, B.; Li, J. Positive Effects of K^+ Ions on Three-Dimensional Mesoporous Ag/Co_3O_4 Catalyst for HCHO Oxidation. *ACS Catal.* **2014**, *4*, 2753–2762. [CrossRef]
21. Zemichael, F.W.; Palermo, A.; Tikhov, M.S.; Lambert, R.M. Propene epoxidation over K-promoted Ag/$CaCO_3$ catalysts: The effect of metal particle size. *Catal. Lett.* **2002**, *80*, 93–98. [CrossRef]
22. Saber, J.M.; Falconer, J.L.; Brown, L.F. Interaction of potassium carbonate with surface oxides of carbon. *Fuel* **1986**, *65*, 1356–1359. [CrossRef]
23. Mims, C.A.; Pabst, J.K. Role of surface salt complexes in alkali-catalysed carbon gasification. *Fuel* **1983**, *62*, 176–179. [CrossRef]
24. Wang, C.; Wang, J.; Wang, J.; Shen, M. Promotional effect of ion-exchanged K on the low-temperature hydrothermal stability of Cu/SAPO-34 and its synergic application with Fe/Beta catalysts. *Front. Environ. Sci. Eng.* **2021**, *15*, 30. [CrossRef]

25. Iwanek, E.; Liotta, L.F.; Williams, S.; Hu, L.; Calilung, L.F.; Pantaleo, G.; Kaszkur, Z.; Kirk, D.W.; Gliński, M. Application of Potassium Ion Deposition in Determining the Impact of Support Reducibility on Catalytic Activity of Au/Ceria-Zirconia Catalysts in CO Oxidation, NO Oxidation, and C_3H_8 Combustion. *Catalysts* **2020**, *10*, 688.
26. Murugadoss, G.; Kumar, D.; Kumar, M.R.; Venkatesh, N.; Sakthivel, P. Silver decorated CeO_2 nanoparticles for rapid photocatalytic degradation of textile rose bengal dye. *Nature* **2021**, *11*, 1080.
27. Ferraria, A.M.; Carapeto, A.P.; Botelho do Rego, A.M. X-ray photoelectron spectroscopy: Silver salts revisited. *Vacuum* **2012**, *86*, 1988–1991. [CrossRef]
28. Nossova, L.; Caravaggio, G.; Couillard, M.; Natis, S. Effect of preparation method on the performance of silver-zirconia catalysts for soot oxidation in diesel engine exhaust. *Appl. Catal. B Environ.* **2018**, *225*, 538–549. [CrossRef]
29. Tudela, D. Silver(II) Oxide or Silver(I,III) Oxide? *J. Chem. Edu.* **2008**, *85*, 863–865. [CrossRef]
30. Cant, N.W.; Fredrickson, P.W. Silver and Gold Catalyzed Reactions of Carbon Monoxide with Nitric Acid and with Oxygen. *J. Catal.* **1975**, *37*, 531–539. [CrossRef]
31. Filtschew, A.; Stranz, D.; Hess, C. Mechanism of NO_2 storage in ceria studied using combined in situ Raman/FT-IR spectroscopy. *Phys. Chem. Chem. Phys.* **2013**, *15*, 9066. [CrossRef] [PubMed]